Title

Comparison of design procedures and observed performance of bridges subjected to lateral spreading

Authors
Turner, Benjamin J
Brandenberg, Scott J
Stewart, Jonathan P

Publication Date
2014-07-01

DOI
10.4231/D3X921K1W

Peer reviewed

Tenth U.S. National Conference on Earthquake Engineering
Frontiers of Earthquake Engineering
July 21-25, 2014
Anchorage, Alaska

COMPARISON OF DESIGN PROCEDURES AND OBSERVED PERFORMANCE OF BRIDGES SUBJECTED TO LATERAL SPREADING

Benjamin Turner[1], Scott J. Brandenberg[2], and Jonathan P. Stewart[3]

ABSTRACT

Recently developed guidelines for analyzing deep foundations in liquefiable soils are compared with the performance of a highway bridge and adjacent railroad bridge that suffered damage during the 2010 M_w 7.2 El Mayor-Cucapah earthquake in Baja California, Mexico. A span of the pile-supported railroad bridge collapsed due to movement of a pier from lateral spreading. The highway bridge, supported on drilled shafts, suffered moderate structural damage but did not collapse. An overview of the site, structural details of the bridges, and results from recent geotechnical explorations characterize the structural properties and soil conditions. Beam on nonlinear Winkler foundation simulations performed using the finite element program OpenSees accurately predict moderate damage to the highway bridge and collapse of the railroad bridge. The case studies provide valuable insight for validating recently published equivalent-static analysis procedures for lateral spreading.

[1]Graduate Student Researcher, Department of Civil and Environmental Engineering, University of California, Los Angeles, bjturner@ucla.edu
[2]Associate Professor and Vice Chair, Department of Civil and Environmental Engineering, University of California, Los Angeles, sjbrandenberg@ucla.edu
[3]Professor and Chair, Department of Civil and Environmental Engineering, University of California, Los Angeles, jstewart@seas.ucla.edu

Turner, B, Brandenberg, SJ, Stewart, JP. Comparison of design procedures and observed performance of bridges subjected to lateral spreading. *Proceedings of the 10th National Conference in Earthquake Engineering*, Earthquake Engineering Research Institute, Anchorage, AK, 2014.

DOI: 10.4231/D3X921K1W

Comparison of Design Procedures and Observed Performance of Bridges Subjected to Lateral Spreading

Benjamin Turner[1], Scott J. Brandenberg[2], and Jonathan P. Stewart[3]

ABSTRACT

Recently developed guidelines for analyzing deep foundations in liquefiable soils are compared with the performance of a highway bridge and adjacent railroad bridge that suffered damage during the 2010 M_w 7.2 El Mayor-Cucapah earthquake in Baja California, Mexico. A span of the pile-supported railroad bridge collapsed due to movement of a pier from lateral spreading. The highway bridge, supported on drilled shafts, suffered moderate structural damage but did not collapse. An overview of the site, structural details of the bridges, and results from recent geotechnical explorations characterize the structural properties and soil conditions. Beam on nonlinear Winkler foundation simulations performed using the finite element program OpenSees accurately predict moderate damage to the highway bridge and collapse of the railroad bridge. The case studies provide valuable insight for validating recently published equivalent-static analysis procedures for lateral spreading.

Introduction

Liquefaction-induced lateral spreading is a complex soil-structure interaction phenomenon capable of causing significant damage to structures during large earthquakes. A synthesis of state-of-the-art research and recommendations for practicing engineers on the topic of designing bridge foundations to resist lateral spreading loads was recently published by the Pacific Earthquake Engineering Research Center (PEER) [1]. A corresponding document published by the California Department of Transportation [2] based on the PEER document provides prescriptive recommendations for design of highway bridges in California.

Damage to a pair of parallel bridges caused by liquefaction and lateral spreading during the 2010 M_w 7.2 El Mayor-Cucapah (EMC) earthquake in northern Baja California, Mexico provides a valuable opportunity to validate the design procedures recommended by [1] and [2]. The Earthquake Engineering Research Institute (EERI) [4] and Geotechnical Extreme Events Reconnaissance (GEER) Association [4] dispatched reconnaissance teams to make detailed post-earthquake observations of the bridges and other effects of the earthquake in the region. Coupled with results of a recent geotechnical site investigation by the authors and structural details of the

[1]Graduate Student Researcher, Department of Civil and Environmental Engineering, University of California, Los Angeles, bjturner@ucla.edu
[2]Associate Professor and Vice Chair, Department of Civil and Environmental Engineering, University of California, Los Angeles, sjbrandenberg@ucla.edu
[3]Professor and Chair, Department of Civil and Environmental Engineering, University of California, Los Angeles, jstewart@seas.ucla.edu

Turner, B, Brandenberg, SJ, Stewart, JP. Comparison of design procedures and observed performance of bridges subjected to lateral spreading. *Proceedings of the 10th National Conference in Earthquake Engineering*, Earthquake Engineering Research Institute, Anchorage, AK, 2014.

bridges, made available by Mexican transportation officials (SCT), the performance of the bridges is compared with the recent guidelines.

Regional Setting

The Mexicali Valley is located in the Salton Trough, a structural depression formed over the last five million years by tension at divergent fault bends along the transform boundary between the Pacific and North American Plates [5]. The basin is filled with sediment from the Colorado River consisting primarily of fine-grained fluvio-deltaic deposits over existing marine, deltaic, lacustrine, and locally derived coarse-grained alluvial fan and fluvial deposits for a total thickness of up to 10-12 km [6, 7]. High groundwater levels from the river and agricultural activity combined with the loose surficial deposits create a high liquefaction hazard throughout the valleys, particularly in recent alluvial floodplain deposits.

Several major earthquakes have occurred in the Mexicali and Imperial Valley region in recent history, including an estimated Mw 7.2 earthquake in 1892 [8]. The April 4, 2010 EMC earthquake occurred on Easter Sunday, with strong shaking felt throughout the region on both sides of the international border [9]. The primarily strike-slip motion caused extensive damage to buildings, utilities, and transportation and agricultural infrastructure [4]. The maximum recorded peak horizontal ground acceleration (PGA) was 0.51 g [8].

San Felipito Bridges

Located approximately 60 km southeast of Mexicali and 14.5 km east of EMC earthquake fault rupture zone (R_{jb}), the San Felipito Bridges (*Puentes de San Felipito*) cross the Colorado River in a relatively flat area flanked by agricultural fields. The river's flood plain is incised approximately five to eight meters below the surrounding topography, separated by steep slopes. The river channel itself is shallow with steep banks.

A railroad bridge and parallel highway bridge span the river's flood plain at the site as shown in Fig. 1. The superstructures of each bridge have much in common—both consist of ten 20-m long spans consisting of precast-prestressed concrete girders simply-supported on elastomeric bearings at the piers and abutments. The spans of each bridge are adjacent such that the piers are aligned as can be seen in Fig. 1, which is likely intended to minimize channel restriction and the hydraulic force acting on the downstream highway bridge piers.

Figure 1. October 2013 site investigation underway at the San Felipito Bridges. Highway bridge is in the foreground; railroad bridge in background. Colorado River, obscured by vegetation, flows under bridges on left side of photo.

The railroad bridge, built in 1962, is supported on monolithic pier walls that flare out to form a pile cap immediately below the ground surface. Although the foundation details for the railroad bridge are unknown, given the date of construction and the river environment, it is likely that the foundations were not designed to resist lateral loads arising from earthquake effects including strong shaking and liquefaction. Each pier of the highway bridge, built in 1998, consist of four 1.2-m diameter extended-shaft columns. The below-grade portions were constructed by advancing a temporary steel casing under its own weight, or by hydraulic jacking in stiff layers, with spoils removed by air-lifting. The casing was withdrawn while concrete was placed using the tremie method [10].

Geotechnical Site Conditions

Subsurface conditions were inferred from a review of the regional and local geology, previous site investigations by SCT, and the results of a detailed site investigation conducted by the authors in October 2013. Portions of boring logs from the original highway bridge site investigation as well as post-earthquake borings for both bridges, including limited index testing results, were provided by SCT.

The subsurface generally consists of interbedded sand and silty sand, with a loose to medium-dense layer to a depth of about 6 to 7 m found near the river and gradually thinning and exhibiting higher relative density further from the river, underlain by 5 to 10 m of alternating dense and loose layers over very dense clean sand. The groundwater table is at a depth of about 1.5 m adjacent to the river. Table 1 presents engineering properties for each layer of the idealized subsurface profile used for the analysis discussed herein. Discretization into the layers presented in Table 1 was focused on the behavior of the subsurface during liquefaction and lateral spreading.

Table 1. Subsurface Profile and Engineering Properties Used for Analysis

Layer	Thickness (m)	Unit Weight (kN/m^3)	Relative Density*	Peak Friction Angle**
1: Unsaturated Silty Sand Crust	1.5	17	55%	35°
2: Loose Sand	5.0	18	42%	35°
3: Dense Sand	1.9	18	77%	40°
4: Medium-Dense Sand	2.8	18	54%	37°
5: Very Dense Sand	> 5	19	82%	41°

* Weighted average using [13], [14], [15]; ** [11, 12]

The authors conducted cone penetration testing (CPT) using a seismic piezocone (SCPTu) with the nees@UCLA truck-mounted Hogentogler CPT rig, capable of pushing to a maximum cone tip resistance of approximately 30 MPa. Three CPT soundings were successfully pushed to refusal at depths ranging between 9.5 and 16.5 m, one CPT was pushed to 4.5 m, and several more tests met refusal at shallow depths due to obstructions. The parameters presented in Table 1 represent an interpretation of the CPT data following the recommendations of [11]. Grain size analysis and Atterberg Limits tests performed on a disturbed bulk sample collected at the surface showed that the fines content of the silty sand is nonplastic silt. The shear wave velocity of the upper soil layers is approximately 100 -220 m/s based on spectral analysis of surface waves (SASW) geophysical testing and seismic CPT cone soundings.

Based on a review of the previous investigations and the results of the recent site investigation, the groundwater level within the vicinity of the bridge appears to closely match the surface elevation of the river. Furthermore, a review of photographs by [4] suggest that the river level immediately following the earthquake was nearly the same as the river level during the authors' October 2013 site investigation. This conveniently eliminates the need to re-interpret the collected data for a different groundwater level.

Ground Failure and Bridge Damage during Earthquake

Lateral spreading cracks were observed on the river banks both north and south of the bridges. The sum of the measured lateral spreading cracks was as much as 4.6 m about 60 m north of the bridge. Measured lateral spreading deformation was greater on the east bank of the river than the west bank, possibly because the river currently flows along the western margin of its floodplain so the alluvial sediments on the east bank are younger and hence looser and more susceptible to liquefaction [16]. This observation could have implications for estimates of potential lateral spreading deformations at similar sites.

Vertical ground settlement on the order of 0.5 to 0.75 m was observed, likely due to a combination of reconsolidation following liquefaction and deviatoric deformation. At the location of the largest measured vertical ground settlement, the highway bridge pier settled vertically approximately 0.5 m due to a bearing capacity failure as a result of loss of resistance in liquefied layers and superposition of static axial loads with down-drag forces mobilized during liquefaction.

Damage to the railroad bridge consisted of collapse of a span adjacent to the east river bank as lateral spreading translated the pier closest to the bank towards the river, leading to unseating of the girders. While the pier moved horizontally about 0.7 m, it displayed only about 0.4 degrees of permanent rotation in the longitudinal direction, barely noticeable with the naked eye. Permanent deformation of the superstructure relative to the piers in the transverse direction was also observed. Similar movement of piers on the west bank of the river nearly led to collapse of two additional spans.

Observed damage to the highway bridge consisted of flexural cracking at the base of the inward (river) side of the columns immediately adjacent to both banks of the river, cracking of shear key "retainers" intended to keep the girders from sliding off the bent cap in the transverse direction, and cracking of the deck due to vertical settlement of one of the piers as discussed above [3, 4]. The flexural cracking at the base of the columns indicates demand towards the center of the river due to lateral spreading and is the primary focus of the analysis described in this paper.

Analysis

An equivalent-static analysis procedure was used to model the bridge behavior under the imposed lateral spreading demand following the recommendations of [1] and [2]. Key aspects of the analysis of the highway bridge will be highlighted in the following sections. Modeling of the railroad bridge was performed by selecting analysis parameters in the same manner as for the highway bridge. Due to space constraints, details of the railroad bridge analysis will not be presented herein, but are included in the final project report to be published by PEER.

Liquefaction Triggering Analysis

A liquefaction susceptibility and triggering analysis for a PGA of 0.24 g was conducted per the recommendations of [14] using the CPT data in order to identify the soil layers presented in Table 1 and to determine the vertical extent of the displaced soil profile depicted in Fig. 2. PGA was estimated by applying the procedures of [17] to the recorded ground motions from nearby strong-motion recording stations.

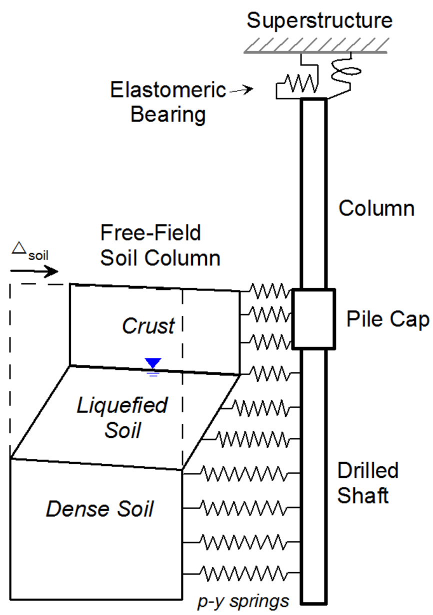

Figure 2. Simplified numerical model of lateral spreading acting on highway bridge extended-shaft column/foundation. Refer to Table 1 for soil profile details.

OpenSees Analysis

The authors used the finite element platform OpenSees [18] to analyze the numerical model shown in Fig. 2. During lateral loading of a pile, behavior of both the structural and geo-materials is nonlinear and it is essential to capture this nonlinearity in order to obtain accurate analysis results. *P-y* spring elements based on the well-known API sand formulation [19] with initial modulus of subgrade reaction based on the relative density values presented in Table 1 represent the nonlinear lateral-load-transfer behavior between the soil and the pile. The *p-y* springs were displaced according to the profile shown in Fig. 3 to simulate lateral spreading loads. The remainder of the analysis was conducted in a manner consistent with programs typically used in practice for analyzing piles under lateral loading such as LPILE [20].

Compared to a non-liquefaction scenario, the load-transfer behavior of the crust layer for a lateral spreading condition is greatly softened due to the presence of the underlying liquefied layer, which is a departure from the typical boundary conditions for passive loading and permits stresses to spread over a larger area [21, 22]. To quantify the lateral-load-transfer between the pile and liquefied soil layers, the estimated resistance of the sand in the non-liquefied condition was reduced by a p-multiplier per the recommendations of [23]. The p-multiplier for the upper liquefied layer was 0.14.

Bridge column and foundation elements were modeled using nonlinear beam-column elements. A bi-linear isotropic hardening material model was used to capture the nonlinear flexural response. In lieu of a more rigorous fiber-section analysis, this approach allows the user to define a single value of effective flexural rigidity (EI_{eff}) representing the cracked section stiffness up to the yield point, and a single value of reduced slope for post-yield behavior. To estimate EI_{eff} and the post-yield slope, the authors first performed a moment-curvature (M-C) analysis of the section using geometric and material properties shown on the construction plans. The post-yield slope and a factor representing the ratio of EI_{eff} to the gross condition (EI_{gross}) were then adjusted using a trial-and-error procedure until the bilinear M-C relationship generated during the OpenSees analysis provided a reasonable match to the estimated M-C behavior from the previous step. The ratio of EI_{eff} / EI_{gross}, which is analogous to the effective stiffness factors for structural elements given in ASCE-41 [24], was found to be approximately 0.2, with a resulting EI_{eff} of about 550 MN*m^2.

Using the bearing dimensions and properties shown on the construction plans, the authors used estimated values of shear and bulk modulus (G = 0.9 MPa and K = 2,000 MPa, respectively, for shore hardness 60 bearings) to compute an effective compression modulus (E_c) per Chapter 14 of the AASHTO LRFD bridge design specifications [25]. Using a computed value of E_c of approximately 12 MPa, the rotational stiffness of the bearing was computed as 60 kN*m/radusing Eq. 1:

$$K_{rotation} = \frac{E_c \times I}{t} \tag{1}$$

Where I is the moment of inertia of the bearing in the bridge longitudinal direction and t is the thickness of the bearing. Shear stiffness of the bearing translational spring was computed as 1,300 kN/m using Eq. 2:

$$K_{shear} = \frac{G \times A}{t} \tag{2}$$

Where A is the cross-sectional area of the bearing and G and t are as defined above. Since each pier has fourteen bearings and four columns, the values of stiffness computed using Eqs. 1 and 2 were multiplied by the ratio [*14/4 = 3.5*] to represent the tributary restraint for a single column.

Inertial demands from the tributary mass of the superstructure were applied to the top of the column as spectral displacement demand as recommended by [1]. These demands can also be imposed as forces following [1] or [2], but the bridge is restrained in the longitudinal direction by the other piers founded in nonliquefied soils and by the abutments, so we selected to impose demands as spectral displacement for this study.

Results

Output from the OpenSees model for a free-field lateral spreading displacement of 1.0 m is shown in Fig. 3. The analysis was repeated for a variety of free-field lateral spreading displacements, and the resulting maximum positive and negative moments developed in the extended shaft column were tabulated. Fig. 4 presents these results as a “pushover curve” for lateral spreading acting on a single pile of the highway bridge pier adjacent to the east river bank. The results show that the moment demand does not increase significantly for free-field lateral spreading displacements in excess of approximately 0.6 m, because the full passive pressure of the crust has been mobilized. Note that the moment demand at large displacement falls between the cracking moment and yield moment for the section, which is consistent with the observation that the columns cracked but did not undergo rotation or displacement indicative of yielding.

Conclusion

The equivalent-static analysis procedure recommended by [1] and [2] has been shown to accurately predict the actual behavior of the highway bridge pier adjacent to the east river bank in terms of moment demand, location of flexural damage, and the deformed shape and magnitude of permanent displacement of the extended-shaft columns. These findings suggest that the ESA procedures are a useful tool for estimating foundation demands in support of design of similar bridges in similar ground conditions. For structurally irregular bridges, complex ground conditions, and major projects, dynamic analysis may still be warranted, but in these cases the ESA can provide a good first approximation of the expected behavior. Final results, including the analysis of the railroad bridge, will be published in a PEER report available in 2014.

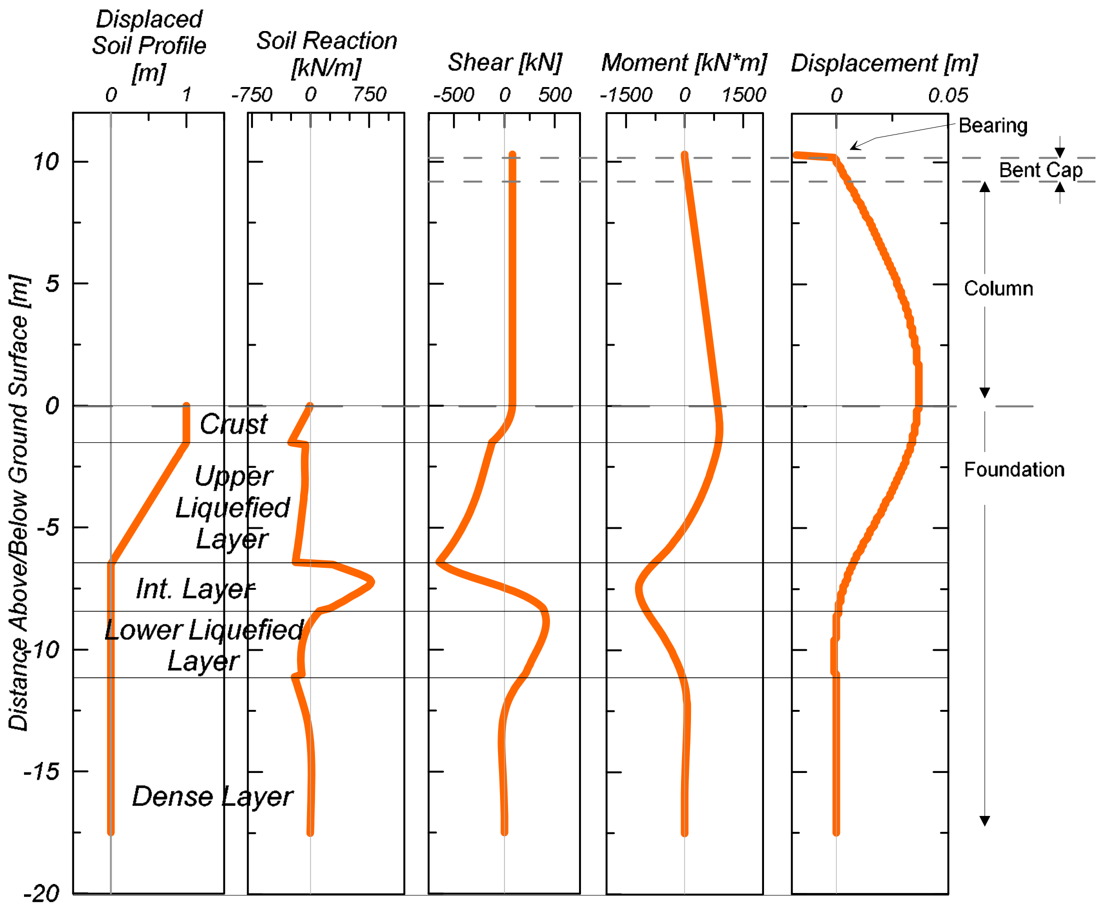

Figure 3. OpenSees model output for a free-field lateral spreading displacement of 1.0 m.

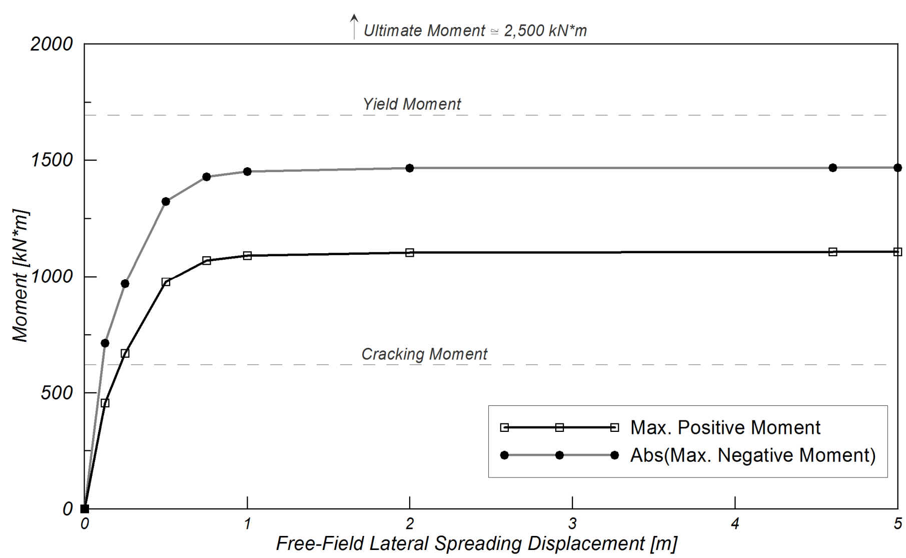

Figure 4. Lateral spreading pushover curve. Maximum positive moment occurs near the ground surface, and maximum negative moment occurs near the interface of the liquefied layer and underlying dense layer.

Acknowledgments

Financial assistance for this project was provided through the PEER Lifelines program. The assistance of SCT officials in coordinating and allowing site access for the investigation is greatly acknowledged, along with the help of Bob Nigbor and Alberto Salamanca of nees@UCLA and Chris Krage of UC Davis during the field work.

References

1. Ashford, S.A., Boulanger, R.W., and Brandenberg, S.J. (2011), "Recommended Design Practice for Pile Foundations in Laterally Spreading Ground," Pacific Earthquake Engineering Research Center, Report No. PEER 2011/04, 44 p.
2. California Department of Transportation (2013), “Guidelines on Foundation Loading and Deformation Due to Liquefaction Induced Lateral Spreading,” Caltrans internal design guideline. Available: http://www.caltrans.ca.gov/research/structures/peer_lifeline_program/docs/Guidelines_on_Foundation_Loading_Due_to_Liquefaction_Oct_16_2013.pdf
3. Meneses, J. (ed.), et al. (2010), “The El Mayor-Cucapah, Baja California Earthquake April 4, 2010, An EERI Reconnaissance Report,” Earthquake Engineering Research Institute, Oakland, California. Available: http://www.eqclearinghouse.org/20100404-baja/general-information/eeri-recon-report
4. Geotechnical Extreme Event Reconnaissance (GEER) (2010) Stewart, J., Brandenberg S. (eds). “Preliminary Report on Seismological and Geotechnical Engineering Aspects of the April 4 2010 M_w 7.2 El Mayor-Cucapah (Mexico) Earthquake”, Report No. GEER-023. Available: http://www.geerassociation.org/GEER_Post%20EQ%20Reports/Baja%20California_2010/Baja_Cover_2010.html
5. McCrink, T.P., Pridmore, C.L., Tinsley, J.C., Sickler, R.R., Brandenberg, S.J., and Stewart, J.P., 2011, Liquefaction and other ground failures in Imperial County, California, from the April 4, 2010, El Mayor–Cucapah earthquake: U.S. Geological Survey Open-File Report 2011–1071 and California Geological Survey Special Report 220, 94 p. pamphlet,1 pl., scale 1:51,440. Available: http://pubs.usgs.gov/of/2011/1071/
6. Merriam, R., & Bandy, O. L. (1965). Source of upper Cenozoic sediments in Colorado Delta region. *Journal of Sedimentary Research*, *35*(4), 911–916. doi:10.1306/74D713A2-2B21-11D7-8648000102C1865D
7. Dorsey, R. J. (2010). Sedimentation and crustal recycling along an active oblique-rift margin: Salton Trough and northern Gulf of California. *Geology*, *38*(5), 443–446. doi:10.1130/G30698.1
8. Hough, S. E. and A. Elliot (2004), “Revisiting the 23 February 1892 Laguna Salada Earthquake,” *Bull. Seis. Soc. Amer.*, **94**(4), 1571-1578.
9. USGS (2010). "Magnitude 7.2 - Baja California, Mexico, 2010 April 04 22:40:42 UTC." Available: http://earthquake.usgs.gov/earthquakes/eqinthenews/2010/ci14607652/.
10. Ramón Pérez Alcalá, Secretaría de Comunicaciones y Transportes México, personal communication, 25 Oct. 2013.
11. Robertson, P. (2012) “Interpretation of in-situ tests—some insights,” Proc. of 4th International Conf. on Geotechnical and Geophysical Site Characterization (ISC-4), Pernambuco, Brazil, September 18-21, R.Q. Coutinho and P.W. Mayne, eds. 22 p.
12. Bolton, M.D., 1986. The strength and dilatancy of sands. *Geotechnique*, **36**(1): 65-78.
13. Zhang, G, PK Robertson, and RW Brachman (2004). "Estimating liquefaction induced lateral displacements using the SPT or CPT," Journal of Geotechnical and Geoenvironmental Engineering, ASCE, 130(8), 861-871.
14. Idriss, IM and RW Boulanger (2008). Soil liquefaction during earthquakes, EERI Monograph MNO-12, EERI, Oakland, CA.

15. Kulhawy, F.H., and Mayne, P.H., 1990. *Manual on estimating soil properties for foundation design*, Report EL-6800, Electric Power Research Institute, EPRI, August 1990.

16. Turner, B., S.J. Brandenberg, and J.P. Stewart (2013). "Evaluation of collapse and non-collapse of parallel bridges affected by liquefaction and lateral spreading," *Proc. 10th International Conf. on Urban Earthquake Engin.*, Center for Urban Earthquake Engineering, March 1-2, 2013, Tokyo Institute of Technology, Tokyo, Japan.

17. Kwak, D.Y., Mikami, A., Brandenberg, S.J., and Stewart, J.P. (2012). Ground motion estimation for evaluation of levee performance in past earthquakes, *Proc. 9th Internationl Conf. on Urban Earthquake Engin.*, Center for Urban Earthquake Engineering, March 6-8, 2012, Tokyo Institute of Technology, Tokyo, Japan.

18. McKenna, F.T. (1997), "Object-Oriented Finite Element Programming: Frameworks for Analysis, Algorithms and Parallel Computing," PhD Thesis, Department of Civil Engineering, University of California, Berkeley.

19. American Petroleum Institute (API), "Recommended Practice for Planning, Designing and Constructing Fixed Offshore Platforms – Working Stress Design", RP 2A-WSD, 20th Edition, July 1, 1993, American Petroleum Institute, Washington, DC

20. Reese, L.C., Wang, S.T., Isenhower, W. M., Arrelaga, J.A., and Hendrix, J. A., 2005. "LPILE Plus Version 5.0," Ensoft, Inc. Austin, TX.

21. Terzaghi, K. (1936). "A fundamental fallacy in earth pressure computations." *J. of the Boston Society of Civil Engineers.* April.

22. Brandenberg, S.J., Boulanger, R.W., Kutter, B.L., Chang, D. (2007a). Liquefaction-induced softening of load transfer between pile groups and laterally spreading crusts, *J. Geotech. Geoenviron. Engrg.,* ASCE, 133(1):91-103.

23. Brandenberg, S.J. (2005). Behavior of pile foundations in liquefied and laterally spreading ground, PhD dissertation, Dept. of Civil and Envir. Engrg., Univ. of Calif., Davis, CA.

24. ASCE/SEI 41-13, 2007, Seismic Rehabilitation of Existing Buildings, American Society of Civil Engineers, Reston, Virginia.

25. AASHTO (2012) LRFD Highway Bridge Design Specifications, American Association of State Highway and Transportation Officials, Washington, D.C., Sixth Edition.